



## OPEN

# In-vivo dark-field and phase-contrast x-ray imaging

## SUBJECT AREAS:

RADIOGRAPHY

DIAGNOSIS

IMAGING TECHNIQUES

APPLIED PHYSICS

M. Bech<sup>1,2</sup>, A. Tapfer<sup>1</sup>, A. Velroyen<sup>1</sup>, A. Yaroshenko<sup>1</sup>, B. Pauwels<sup>3</sup>, J. Hostens<sup>3</sup>, P. Bruyndonckx<sup>3</sup>, A. Sasov<sup>3</sup> & F. Pfeiffer<sup>1</sup><sup>1</sup>Physics Department & Institute for Medical Engineering, Technische Universität München, 85748 Garching, Germany, <sup>2</sup>Medical Radiation Physics, Lund University, 221 85 Lund, Sweden, <sup>3</sup>Bruker microCT, Kartuizersweg 3B, B-2550 Kontich, Belgium.Received  
4 June 2013Accepted  
29 October 2013Published  
13 November 2013Correspondence and  
requests for materials  
should be addressed to  
F.P. (franz.pfeiffer@  
tum.de)

**Novel radiography approaches based on the wave nature of x-rays when propagating through matter have a great potential for improved future x-ray diagnostics in the clinics. Here, we present a significant milestone in this imaging method: in-vivo multi-contrast x-ray imaging of a mouse using a compact scanner. Of particular interest is the enhanced contrast in regions related to the respiratory system, indicating a possible application in diagnosis of lung diseases (e.g. emphysema).**

**P**hase-contrast radiography approaches based on the wave-like behavior of x-rays in matter provide complementary image information to the conventional x-ray image, opening for the possibility to significantly impact x-ray diagnostics in the clinics. Of the different approaches to obtain such new images, a recently developed technique, based on micro-structured x-ray transmission gratings, appears particularly promising; it works not only with large-scale synchrotron facilities, but also with conventional x-ray tube sources<sup>1–4</sup>. Several groups worldwide are presently making an effort to translate such multi-contrast x-ray imaging from bench to bedside<sup>5–9</sup>.

Though several technical challenges still need to be overcome before clinical implementation is possible (such as increased mechanical stability and fabrication of large-area, high-quality wave-optical x-ray gratings), the first step in this direction is the development of a small-animal prototype scanner where the ‘patient’ lies on a bed. At this stage, more basic questions about the medical relevance of the new imaging modalities can be addressed. Currently, efforts are undertaken to evaluate for which radiological application the method will provide the largest additional diagnostic value, and studies of lung disease development in living animals are in progress. Previously published ex-vivo data includes two studies with a grating interferometer using a laser-driven x-ray source: A proof-of-principle emphysema diagnosis<sup>10</sup>, and a receiver-operating-characteristic curve analysis to evaluate the diagnostic value of each image channel in differentiating between healthy and emphysematous lung tissue<sup>11</sup>. Further, the method has recently been translated to proof-of-principle imaging with the compact scanner also used in the current study<sup>12</sup>.

## Results

Here, we present a set of complementary x-ray images successfully acquired of a living mouse. These results were obtained with a multi-contrast x-ray small-animal imaging scanner, which we have recently developed and commissioned<sup>13,14</sup>. Figure 1 displays the three components of the multi-contrast x-ray image acquired. The three images in Figure 1 are acquired simultaneously, and show two new imaging signals – the differential phase-contrast radiograph, based on refraction (Fig. 1b), and the dark-field contrast radiograph, based on scattering (Fig. 1c) – alongside with the conventional x-ray image, based on attenuation (Fig. 1a).

The multi-contrast image is formed by exploiting the wave nature of x-rays. Whether the x-ray photons are absorbed, coherently refracted or scattered, the interaction can be used to form an image. To extract this information, three x-ray transmission gratings are located in the x-ray beam path: one behind the source, one behind the specimen and one right in front of the detector. Together they form an interferometer, producing an interference pattern, which is analyzed to retrieve the multi-contrast x-ray image with three different contrast channels. A schematic view of the experiment is displayed in the Supplementary Figure 1. Inherently, the three contrast channels have the same resolution, and they are perfectly registered pixel by pixel. In the imaging process, a so-called phase-stepping scan is performed, by acquiring five exposures with slightly different relative positions of the interferometer gratings<sup>3</sup>. Subsequently the three image modalities are extracted from the recorded frames

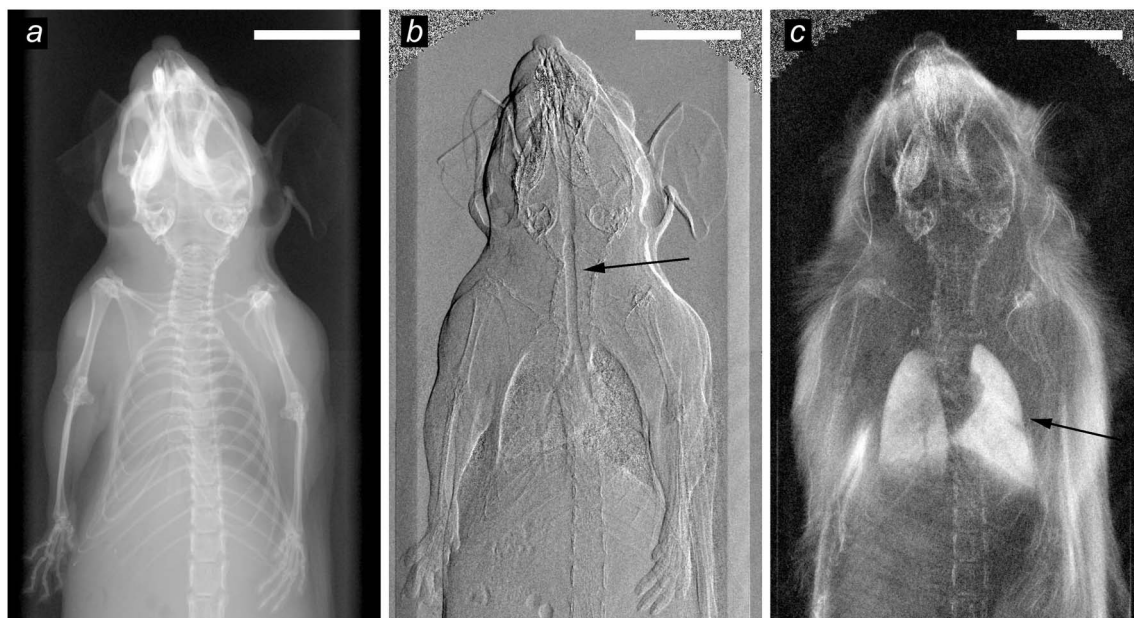


**Figure 1 | First in-vivo multi-contrast x-ray images of a mouse.** (a) Conventional x-ray image based on attenuation. (b) Differential phase-contrast image based on x-ray refraction. (c) Dark-field image based on x-ray scattering. All three images are intrinsically perfectly registered as they are extracted from the same data recorded with a grating interferometer. Examples of regions of enhanced contrast are marked with arrows, showing the refraction of the trachea (b) and the scattering of the lungs (c). The white bars correspond to 1 cm.

by fast Fourier computer processing. Finally, the resulting images are normalized and any residual phase ramp is removed from the differential phase image<sup>14</sup>.

As illustrated, the information gained from each of the three contrast modalities is of complementary nature. The conventional x-ray image (Fig. 1a) shows very good contrast between bones and soft tissue, mainly due to the increased x-ray attenuation of calcium compared to the lighter organic elements. The differential phase-contrast image (Fig. 1b) enhances details in the soft tissue<sup>1</sup>. In particular the interfaces of air filled regions are clearly shown, such as the trachea (marked by an arrow) or the lungs. For the sake of direct comparison and to highlight the complementary information encoded in those two signals, the differential phase-contrast image is displayed side-by-side with the differential attenuation image in Supplementary Figure 2 online. Finally, The dark-field image (Fig. 1c) enhances features containing sub-pixel-sized micro-structures because of ultra small-angle x-ray scattering<sup>3,15–17</sup>. Particularly the lungs exhibit a strong signal, as their main morphological structures – the alveoli – have a typical size of a few ten micrometers<sup>10</sup>.

## Discussion

Although the mouse used for this demonstration does not carry any diseases, it is evident from the radiographs (Fig. 1), that multi-contrast x-ray imaging offers a great potential for added value in clinical x-ray diagnostics. Moreover, the results demonstrate that even though some blurring occurs due to heart beat and breathing cycles (as is also the case in conventional x-ray and tomography images of small animals), this motion does not lead to a break-down of the phase- or dark-field contrast images in-vivo, as is currently controversially discussed in the scientific community.

In summary, the images we have presented are the result of a dedicated effort in the development of a compact scanner for phase-contrast and dark-field x-ray imaging of small animals in a standard laboratory. This marks a milestone towards multi-contrast x-ray radiography in a pre-clinical setting. The first in-vivo results on small rodents particularly highlight improved contrast in regions related to the respiratory system, making application in diagnosis of lung diseases (e.g. emphysema) possible. Future work will focus on

evaluating the added clinical benefit for several small animal disease models (including spontaneous cancer models of different organs), also employing computed tomography.

## Methods

The images were recorded with a Talbot-Lau x-ray interferometer<sup>1</sup> with three gratings: Source grating and analyzer grating have gold structures approximately 35  $\mu\text{m}$  deep, with grating pitch of 10.0  $\mu\text{m}$  and 4.8  $\mu\text{m}$  respectively. The phase grating has 4.0  $\mu\text{m}$  deep nickel structures with a pitch of 3.24  $\mu\text{m}$ . All gratings structures have a duty cycle of 0.5. The x-ray source is a 50 Watt tungsten tube (RTW, MCBM 65B) with a 50  $\mu\text{m}$  focal spot size, and the detector is a Hamamatsu flat panel (C9312SK-06). The x-ray tube was operated at 31 kV peak voltage and 500  $\mu\text{A}$  current during the experiment. The interferometer (total length approximately 470 mm) is mounted in a gantry allowing a vertical beam path through the mouse specimen lying on the sample bed. Five images were acquired with a 10 seconds exposure each, giving a total dose of 3.9 mGy to the animal. The raw images were Fourier processed and ramp corrected to obtain the three image modalities. Finally two regions of interest were stitched together, giving the result presented in Fig. 1. The study protocol was approved by the Ethics Committee for animal studies of the University of Antwerp.

- Pfeiffer, F., Weitkamp, T., Bunk, O. & David, C. Phase retrieval and differential phase-contrast imaging with low-brilliance X-ray sources. *Nat. Phys.* **2**, 258–261 (2006).
- Pfeiffer, F., Kottler, C., Bunk, O. & David, C. Hard x-ray phase tomography with low-brilliance sources. *Phys. Rev. Lett.* **98**, 1–4 (2007).
- Pfeiffer, F. *et al.* Hard-x-ray dark-field imaging using a grating interferometer. *Nat. Mater.* **7**, 134–137 (2008).
- Bech, M. *et al.* Quantitative X-ray dark-field computed tomography. *Phys Med Biol.* **55**, 5529–5539 (2010).
- Bennett, E. E., Kopace, R., Stein, A. F. & Wen, H. A grating-based single-shot x-ray phase contrast and diffraction method for in vivo imaging. *Med. Phys.* **37**, 6047–6054 (2010).
- Stutman, D., Beck, T. J., Carrino, J. A. & Bingham, C. O. Talbot phase-contrast x-ray imaging for the small joints of the hand. *Phys. Med. Biol.* **56**, 5697–5720 (2011).
- Itoh, H. *et al.* X-ray phase-contrast imaging using Fourier transform phase retrieval. *Opt. Expr.* **19**, 3339–3346 (2011).
- Stampanoni, M. *et al.* The first analysis and clinical evaluation of native breast tissue using differential phase-contrast mammography. *Invest. Rad.* **46**, 801–806 (2011).
- Kiyohara, J. *et al.* Development of the Talbot-Lau interferometry system available for clinical use. *AIP Conf. Proc.* **1466**, 97–102 (2012).
- Schleede, S. *et al.* Emphysema diagnosis using x-ray dark-field imaging at a laser-driven compact synchrotron light source. *Proc. Nat. Acad. Sci. USA.* **109**, 17880–17885 (2012).



11. Meinel, F. *et al.* Diagnosing and Mapping Pulmonary Emphysema on X-Ray Projection Images: Incremental Value of Grating-Based X-Ray Dark-Field Imaging. *PLoS ONE*. **8**, e59526 (2013).
12. Yaroshenko, A. *et al.* Pulmonary Emphysema Diagnosis with a Preclinical Small-Animal X-ray Dark-Field Scatter-Contrast Scanner. *Radiology*. doi:10.1148/radiol.13122413 (2013).
13. Tapfer, A. *et al.* Development of a prototype gantry system for preclinical x-ray phase-contrast computed tomography. *Med. Phys.* **38**, 5910–5915 (2011).
14. Tapfer, A. *et al.* Experimental results from a preclinical x-ray phase-contrast CT scanner. *Proc. Nat. Acad. Sci. USA*. **109**, 15691–15696 (2012).
15. Yashiro, W., Terui, Y., Kawabata, K. & Momose, A. On the origin of visibility contrast in x-ray Talbot interferometry. *Opt. Expr.* **18**, 16890–16901 (2010).
16. Lynch, S. K. *et al.* Interpretation of dark-field contrast and particle-size selectivity in grating interferometers. *Appl. Opt.* **50**, 4310–4319 (2011).
17. Chen, G. H., Bevins, N., Zambelli, J. & Qi, Z. Small-angle scattering computed tomography (SAS-CT) using a Talbot-Lau interferometer and a rotating anode x-ray tube: theory and experiments. *Opt. Expr.* **18**, 12960–12970 (2010).

## Acknowledgments

M.B., A.T., A.V., A.Y. and F.P. acknowledge financial support through the DFG Cluster of Excellence Munich-Center for Advanced Photonics (MAP), the DFG Gottfried Wilhelm Leibniz program and the European Research Council (FP7, Starting grant #240142). The work was partly carried out with the support of the Karlsruhe Nano Micro Facility (KNMF;

www.kit.edu/knmf), a Helmholtz Research Infrastructure at Karlsruhe Institute of Technology (KIT; www.kit.edu). A.T., A.V. and A.Y. acknowledge the TUM Graduate School for the support of their studies. The authors thank P. Thibault for helping to improve the manuscript.

## Author contributions

F.P. and A.S. initiated and coordinated the project. F.P., M.B., B.P., P.B. and A.S. conceived the grating interferometer and scanner hardware. A.T., A.V., A.Y., B.P. and M.B. commissioned the scanner. A.V., A.Y., B.P. and J.H. performed the experiment. M.B. treated the data and wrote the manuscript text. All authors reviewed the manuscript.

## Additional information

Supplementary information accompanies this paper at <http://www.nature.com/scientificreports>

**Competing financial interests:** The authors declare no competing financial interests.

**How to cite this article:** Bech, M. *et al.* In-vivo dark-field and phase-contrast x-ray imaging. *Sci. Rep.* **3**, 3209; DOI:10.1038/srep03209 (2013).



This work is licensed under a Creative Commons Attribution-NonCommercial-NoDerivs 3.0 Unported license. To view a copy of this license, visit <http://creativecommons.org/licenses/by-nc-nd/3.0>